Microwave spectroscopy of the Schmid transition

Manuel Houzet[1], Tsuyoshi Yamamoto[2], and Leonid I. Glazman[3]
[1]*Univ. Grenoble Alpes, CEA, Grenoble INP, IRIG, PHELIQS, 38000 Grenoble, France*
[2]*Faculty of Pure and Applied Physics, University of Tsukuba, Tsukuba, Ibaraki 305-8571, Japan*
[3]*Department of Physics, Yale University, New Haven, Connecticut 06520, USA*

(Received 5 September 2023; revised 27 February 2024; accepted 4 March 2024; published 24 April 2024)

Schmid transition was introduced first as a superconductor-insulator transition in the zero-frequency response of a shunted Josephson junction in equilibrium at zero temperature. As it is typical for a quantum impurity problem, at finite frequencies the transition is broadened to a crossover. Modern attempts to find Schmid transition rely on finite-frequency measurements of a quantum circuit. We predict the frequency dependence of the admittance and reflection phase shift for a high-impedance transmission line terminated by a Josephson junction for a wide variety of devices, from a charge qubit to a transmon. Our results identify the circuit parameters needed for the experimental observation of universal scaling of the responses with frequency. On the insulating side of the transition, the full crossover from weak to strong coupling can only be observed in a transmon. On the contrary, observation of such crossover on the superconducting side of the transition is possible only with the charge qubit. The frequency dependence gets weaker and vanishes upon approaching the Schmid transition from either side.

DOI: 10.1103/PhysRevB.109.155431

I. INTRODUCTION

The Schmid transition predicts that the ground-state wavefunction associated with a quantum-mechanical particle placed in a periodic potential is either localized or extended, depending of the strength of its coupling with a dissipative environment [1]. The existence of the transition was supported by a duality transformation between the two phases [1] and confirmed with renormalization-group (RG) calculations [2,3]. Furthermore, RG methods allow to argue that the transition only depends on the properties of the environment, not on the amplitude of the periodic potential.

The particle in the Schmid transition can be associated with the phase across a Josephson junction shunted by a resistor. If its resistance R is smaller than the resistance quantum, $R < h/4e^2$, then the phase is localized in one of the minima of the Josephson potential. Conversely, on the other side of the transition, $R > h/4e^2$, the phase is delocalized and the junction behaves as an insulator [2,3]. So far, the phase diagram experimentally inferred from the dc response of shunted Josephson devices [4,5] is far from reproducing the predicted phase diagram.

Modern attempts to observe the Schmid transition rely on finite-frequency [6–8] and related heat transport [9] measurements of a superconducting circuit.

As it is typical for a quantum impurity problem, a finite temperature or frequency broadens the quantum phase transition into a crossover. The effect of thermal fluctuations received early attention [10,11]. Much less is known on the role of a finite frequency that was mostly studied in perturbative regimes [12–16].

In this paper we develop the theory of finite-frequency response functions needed for a correct interpretation of experimental data. Our results identify the circuit parameters allowing for the universal scaling of the responses with the frequency, and determine the frequency range where scaling laws apply. We predict the frequency dependence of the reflection phase shift for a high-impedance transmission line terminated by a Josephson junction, see Fig. 1(a), for a wide variety of devices, from a transmon ($E_J \gg E_C$) to a charge qubit ($E_J \ll E_C$). We relate the phase shift with the admittance for the circuit in Fig. 1(b). Here E_J is the Josephson energy and $E_C = e^2/2C$, where C is the junction capacitance, is the charging energy.

II. MODEL

The Hamiltonian that describes a circuit formed of a Josephson junction in series with a transmission line is

$$H = E_J(1-\cos\varphi) + 4E_C(N-n-\mathcal{N})^2 + \sum_q \omega_q a_q^\dagger a_q. \quad (1)$$

Here N is the charge (in units of $2e$) that flows across the junction and φ is the canonically conjugate superconducting phase difference. The charge displaced from the transmission line to the junction,

$$n = \frac{1}{\pi}\sum_q \sqrt{\frac{K\Delta}{\omega_q}}(a_q + a_q^\dagger), \quad (2)$$

is related with the boson annihilation operator a_q for a mode with energy $\omega_q = (q+\frac{1}{2})\Delta$ (q positive integer) in the transmission line when it is shorted on the junction side and open on the opposite side. Here $\Delta = \pi v/L$ is the mean level spacing in a transmission line of finite length L, characterized by velocity v and line impedance $R = \pi\hbar/4e^2K$ (such that the Schmid transition occurs at $K = \frac{1}{2}$). To describe the circuit of

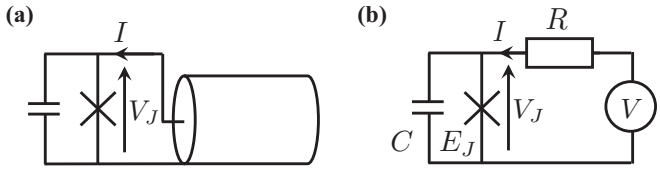

FIG. 1. Two equivalent circuits. (a) A transmission line terminated by a Josephson junction and (b) a voltage driven Josephson junction in series with a resistor.

Fig. 1(b), we take the limit $L \to \infty$ and introduce the voltage bias $V = 2e\dot{\mathcal{N}}R$ with the drive variable $\mathcal{N}$.

The coupling between the junction and the line modifies the scattering properties of bosons incident from the line. In general, bosons scatter inelastically off the junction due to its nonlinearity. Still, the elastic part of the scattering matrix can be related with the circuit admittance $Y(\omega)$ at frequency ω. In the one-port setup that we consider, this part reduces to the reflection amplitude $r(\omega) = e^{2i\delta(\omega)}$, with complex scattering phase $\delta(\omega) = \delta'(\omega) + i\delta''(\omega)$. Indeed, in linear response we find

$$Y(\omega) \equiv \frac{I(\omega)}{V(\omega)} = \frac{1}{2R}(1 - e^{2i\delta(\omega)}), \tag{3}$$

where $I = (V - V_J)/R$ is the current flowing through the junction and V_J is the voltage at the junction, see details in Appendix A. Using the classical formula for adding impedances in series, $1/Y = R + 1/Y_J$, we define the effective junction admittance,

$$Y_J(\omega) \equiv \frac{I(\omega)}{V_J(\omega)} = (-i/R)\tan\delta(\omega). \tag{4}$$

Note that $\delta(\omega)$ is defined modulo π; for convenience we fix it such that $0 < \delta'(\omega) < \pi$. Equation (4) shows that the reflection is elastic [$\delta(\omega)$ is real] when $Y_J(\omega)$ is purely reactive, while the inelastic cross section, $\sigma_{\rm in}(\omega) = 1 - |r(\omega)|^2$, is finite if $Y_J'(\omega) \neq 0$.

The microwave spectroscopy of a finite-length transmission line that is open on one side, such that $V_{\rm in}(\omega) = e^{2i\omega L/v}V_{\rm out}(\omega)$, and closed by a Josephson junction on the other side, provides a direct way of measuring $\delta(\omega)$. Indeed, from the closure condition $e^{-2i\omega L/v} = e^{2i\delta(\omega)}$ we find that, when inelastic scattering is small, the frequency shift of the standing modes is $\delta\omega_n = \Delta[1/2 - \delta'(\omega_n)/\pi]$, while $\sigma_{\rm in}(\omega)$ yields an internal contribution to the mode's quality factor, $Q(\omega_n) = 2\pi\omega_n/\Delta\sigma_{\rm in}(\omega_n)$. This method has been implemented in a variety of experiments aiming at studying many-body physics with microwave photons in Josephson-junction arrays [7,8,17–22].

Based on these relations, one expects [8] that, in the zero-frequency limit, the Schmid transition between the superconducting phase ($K > \frac{1}{2}$) and the insulating phase ($K < \frac{1}{2}$) manifests itself by a $\pi/2$ phase shift in the amplitude of wave reflection off the junction. Indeed, in the superconducting phase, the low-frequency response of the junction is inductive, such that $r = -1$ and $Y = 1/R$; in the insulating phase, the low-frequency response of the junction is capacitive, such that $r = 1$ and $Y = 0$.

Clearly, the zero-frequency limit is of little use for the interpretation of microwave experiments. On the other hand, not so much is known about the response at finite frequencies. Below we make specific predictions, focusing mostly on the scaling (universal) regimes. First, we recall two simple limits, $K \gg 1$ and $K \ll 1$, respectively. Their analysis will help us determine the domain of parameters where one may expect large variations of the phase shift with the frequency.

We first consider the classical limit, $K \gg 1$. Here $Y_J(\omega) = i/\omega L_J$ with Josephson inductance $L_J = 1/4e^2E_J$ at any ω up to the plasma frequency, $\omega_0 = \sqrt{8E_JE_C}$, except in a narrow vicinity of ω_0 on the order of the plasma resonance linewidth, $2\Gamma \equiv 1/RC$. Thus $\delta(\omega) \approx \pi/2$ hardly depends on ω in a transmon. On the other, in a charge qubit $\delta(\omega)$ varies by $\sim\pi/2$, increasing with ω from $\pi/2$ to π in the frequency range $\omega \ll \Gamma$. The increase by $\pi/2$ occurs on the scale $\omega \sim R/L_J \ll \Gamma$.

Then we consider the opposite limit of an almost disconnected Josephson junction, $K \ll 1$. Here the low-frequency response is determined by an effective capacitance $C_\star$, $Y_J(\omega) = -i\omega C_\star$, where $C_\star$ is fixed by the sensitivity of the ground-state energy to an external gate voltage in a disconnected device, $K = 0$ [23] (see also Appendix B 1). In particular, in a charge qubit, such low-frequency response holds with $C_\star \approx C$ at $\omega \ll E_C$. As a result, $\delta(\omega) \approx 0$ hardly depends on the frequency if $\omega \ll \Gamma$. On the other hand, the capacitive response of a transmon holds with $C_\star = e^2/\pi^2\lambda$ if $\omega \ll \sqrt{\lambda E_J}$, see details in Appendix B 2. Here

$$\lambda \approx \frac{8}{\sqrt{\pi}}\left(8E_J^3E_C\right)^{1/4}e^{-\sqrt{8E_J/E_C}} \ll \omega_0 \tag{5}$$

is the phase slip amplitude. As a result, $\delta(\omega)$ largely deviates from 0 in a frequency range $\ll \omega_0$. It actually increases by $\pi/2$ as the frequency crosses over the scale $K\lambda$. Let us emphasize that this crossover is a purely single-particle, albeit nonlinear, effect and has nothing to do with many-body physics.

Overall, the above results show that the variation of the phase by $\pi/2$ occurs in opposite limits ($K \gg 1$ and $K \ll 1$) for the charge qubit and transmon. Away from these limits, many-body effects modify this crossover and result in a universal scaling behavior for the reflection phases. Below we will argue that the variation of $\delta(\omega)$ by $\pi/2$ in a charge qubit at $K > 1/2$ is described by a complex, K-dependent scaling function,

$$\delta(\omega) = f_{\rm qb}(\omega/\Omega_\star, K), \tag{6}$$

as the frequency crosses over a characteristic frequency $\Omega_\star$. Correspondingly, we will determine the complex scaling function for the variation of reflection phase

$$\delta(\omega) = f_{\rm tr}(\omega/\omega_\star, K) \tag{7}$$

in a transmon at $K < 1/2$ with another characteristic frequency $\omega_\star$.

III. FINITE-FREQUENCY RESPONSE OF A CIRCUIT TERMINATED BY A TRANSMON

Let us start with the transmon coupled to a transmission line. Starting from Eq. (1), we find that the low-energy

properties of the circuit are described by a boundary sine-Gordon Hamiltonian

$$H = H_0 - \lambda \cos(2\theta(0) + 2\pi\mathcal{N}),$$
$$H_0 = \int_0^\infty dx \left[\frac{vK}{2\pi}(\partial_x\varphi)^2 + \frac{v}{2\pi K}(\partial_x\theta)^2 \right], \tag{8}$$

defined in a bandwidth of the order of ω_0 (its precise value is beyond the accuracy of our considerations, see Appendix B 3 for details). The Hamiltonian H_0, which appears as the last term in Eq. (1) in the eigenmode representation, is written here in terms of the canonically conjugate phase $[\varphi(x)]$ and charge $[\frac{1}{\pi}\partial\theta(x)]$ variables, $[\varphi(x), \frac{1}{\pi}\partial_x\theta(x')] = i\delta(x-x')$. The charge displaced to the transmon, which determines the current operator, is $2e(n+\mathcal{N})$ with $n = \frac{1}{\pi}\theta(0)$. The second term in Eq. (8) describes the phase slips at the Josephson junction. Using linear response and the equations of motion derived from Eq. (8), see Appendix C 1, we find

$$Y(\omega) = \frac{1}{R}[1 - 4\pi K\mathcal{G}(\omega)] \tag{9}$$

with

$$\mathcal{G}(\omega) = \frac{\lambda^2}{-i\omega}[G_{\sin 2\pi n, \sin 2\pi n}(\omega) - G_{\sin 2\pi n, \sin 2\pi n}(\omega = 0)]. \tag{10}$$

Here we introduced retarded Green's functions $G_{A,B}(t) = -i\theta(t)\langle[A(t), B]\rangle$ for operators A, B, and the last term in Eq. (10) arises from the relation [14]

$$\langle \cos 2\pi n\rangle = -\lambda G_{\sin 2\pi n, \sin 2\pi n}(\omega = 0). \tag{11}$$

Equations (10) and (11) are valid at any λ.

At $K > 1/2$ the second term in H of Eq. (8) is irrelevant. It is easy to show that $\delta(\omega)$ remains small at any ω by using Eq. (3) and treating λ perturbatively in Eq. (9) [24].

At $K < \frac{1}{2}$, the perturbative-in-λ result can be cast in the form (see Appendix C 2 for details)

$$\delta(\omega) = \frac{\pi}{2} + [\tan 2\pi K + i]\left(\frac{\omega_\star}{\omega}\right)^{2-4K}. \tag{12}$$

The frequency-dependent correction remains small only at large frequencies, $\omega \gg \omega_\star$. Here we introduced the crossover frequency

$$\omega_\star = \omega_0 \left(\sqrt{\frac{2K}{\Gamma(4K)}} \frac{\pi\lambda}{\omega_0} \right)^{1/(1-2K)}, \tag{13}$$

below which the RG flow points towards the strong-coupling regime of the boundary sine-Gordon model [3]. The negative sign of $\delta'(\omega) - \frac{\pi}{2} \propto \tan 2\pi K$ in Eq. (12) corresponds to a capacitive response with an effective ω-dependent capacitance. A finite value of $\delta''(\omega)$ corresponds to a finite inelastic cross section. Its frequency dependence reflects a quasielastic process similar to the one displayed by quasiresonant photons [25,26], see Appendix B 4 for details at $K \ll 1$.

In order to go beyond perturbation theory and address the low-frequency response, $\omega \ll \omega_\star$, we use a Hamiltonian dual to Eq. (8),

$$H = H_0 - \tilde{\lambda}\cos\varphi(0) - \dot{\mathcal{N}}\varphi(0). \tag{14}$$

To motivate it, we note that the failure of perturbation theory at low frequency could be ascribed to the effective pinning of the charge $\theta(0)$ to multiples of π (in absence of drive). The term $\propto \tilde{\lambda}$ in Eq. (14) accounts for the slips induced by quantum fluctuations between those different pinned states. The precise relation of $\tilde{\lambda}$ to λ,

$$\frac{\pi\tilde{\lambda}}{\omega_0} = \frac{\Gamma(1/2K)}{2K}\left(\frac{1}{2K\Gamma(2K)}\frac{\pi\lambda}{\omega_0}\right)^{-1/2K}, \tag{15}$$

was found in Ref. [27]. Overall, Eq. (14) takes the same form as the Hamiltonian for a driven Josephson junction in series with a resistor. Using linear response and the equations of motion derived from Eq. (14), we may find a relation between the admittance and $\varphi(0)$-correlation functions valid at any $\tilde{\lambda}$. As the Josephson term in Eq. (14) is irrelevant at $K < \frac{1}{2}$, a perturbative-in-$\tilde{\lambda}$ expansion of the admittance will be valid down to the lowest frequencies. Using Eq. (3) to relate it with the frequency shift, we may express the result obtained up to $\tilde{\lambda}^2$ as

$$\delta(\omega) = \tilde{c}(1/4K)\tilde{c}^{1/2K}(K)[\tan(\pi/2K) + i]\left(\frac{\omega}{\omega_\star}\right)^{1/K-2} \tag{16}$$

with $\tilde{c}(K) = 8K^3\Gamma^2(2K)/\Gamma(4K)$, see details of the derivation in Appendix C 3. We note that the negative sign of $\delta'(\omega) - \frac{\pi}{2} < 0$ still corresponds to a capacitive response.

The power-law frequency scaling in Eqs. (12) and (16) mirrors the celebrated bias dependence of nonlinear conductance in the Kane-Fisher theory [14] of Luttinger liquid transport across a quantum impurity. It also matches the frequency dependencies of the conductance, which are given in the Appendix of Ref. [14] at weak and strong coupling, respectively. In addition, the K-dependent prefactors in Eqs. (12) and (16) *uniquely relate* the strong coupling response to the weak-coupling one (not just the power-law exponents) in the same device. The inclusion of the nondissipative part $[\delta'(\omega)]$ in the response shows the need to modify Eqs. (12) and (16) at small K.

Indeed, the amplitude of the nondissipative term in Eq. (16) diverges at $K = \frac{1}{3}$, and $\delta'(\omega)$ exhibits a "super-capacitive" response at $K < \frac{1}{3}$: the exponent $\alpha = 1/K - 2$ of its ω dependence *exceeds* the value $\alpha = 1$ of a disconnected transmon. It indicates that, at $K < \frac{1}{3}$ and $\omega \ll \omega_\star$ the capacitive response originates from another irrelevant term $c_2[\partial_x\theta(0)]^2$, which needs to be added to the effective low-energy Hamiltonian (14). It accounts for the quantum fluctuations of the charge $\theta(0)$ in vicinity of a given pinned state. Such term was introduced phenomenologically in [15,16]. The expression for the coefficient c_2 in terms of K, λ, ω_0 was found as a part of series of irrelevant terms $\sum_{n=1}^\infty c_{2n}[\partial_x\theta(0)]^{2n}$ developed in [28,29]. By accounting for the term $c_2[\partial_x\theta(0)]^2$ in evaluation [30] of $\delta(\omega)$ we find

$$\delta(\omega) = \frac{\omega}{\beta(K)\omega_\star} + i\tilde{c}(1/4K)\tilde{c}^{1/2K}(K)\left(\frac{\omega}{\omega_\star}\right)^{1/K-2},$$
$$\frac{1}{\beta(K)} = \frac{1}{2\sqrt{\pi}}\Gamma\left(\frac{1/2}{1-2K}\right)\Gamma\left(\frac{1-3K}{1-2K}\right)\left(\frac{\tilde{c}(K)}{4K^2}\right)^{\frac{1}{2(1-2K)}}. \tag{17}$$

Note that the effective capacitance here, $\sim 1/\beta(K)$, depends nontrivially [31] on K. Remarkably, $\beta(0) = \sqrt{2}$ allowing one to recover $C_\star$ found at $\omega/\omega_\star \ll 1$ in the isolated-transmon ($K \ll 1$) limit, see Eq. (5).

Next we notice that the nondissipative term in Eq. (12) diverges at $K = \frac{1}{4}$, and $\delta'(\omega)$ exhibits a "super-capacitive" response at $K < \frac{1}{4}$. The leading $1/\omega$ asymptote of $\delta'(\omega)$ comes, instead, from the second term in Eq. (10),

$$\delta(\omega) = \frac{\pi}{2} - \frac{\alpha(K)\omega_\star}{\omega} + i\left(\frac{\omega_\star}{\omega}\right)^{2-4K} \tag{18}$$

with $\alpha(K)\omega_\star = 4\pi K\lambda\langle\cos 2\pi n\rangle$. We find the precise dependence

$$\alpha(K) = \frac{2}{\sqrt{\pi}}\Gamma\left(\frac{\frac{1}{2}-2K}{1-2K}\right)\Gamma\left(\frac{1-K}{1-2K}\right)\left(\frac{4K^2}{\tilde{c}(K)}\right)^{\frac{1}{2(1-2K)}} \tag{19}$$

by using the exact result for $\langle\cos 2\pi n\rangle$ for the boundary sine-Gordon model at $K < \frac{1}{4}$ [33]. Reassuringly, $\alpha(0) = \sqrt{2}$, so that $C_\star$ of an almost-isolated transmon is also recovered at $\omega/\omega_\star \gg 1$ and $K \to 0$.

Inspecting the capacitive terms in Eqs. (12) and (18), we find with the help of Eq. (19) that the amplitude of $\delta'(\omega)$ diverges at $K - \frac{1}{4} \to \pm 0$. The special point $K = \frac{1}{4}$ corresponds to the Toulouse limit [14,34], which provides an exact result covering the crossover at $\omega_\star$ [8] (see also Appendix C 4),

$$\frac{e^{2i\delta(\omega)}+1}{2} = \frac{2\omega_\star}{i\pi\omega}\ln\left(1 - \frac{i\pi\omega}{2\omega_\star}\right), \quad \omega_\star = \frac{\pi^2\lambda^2}{2\omega_0}. \tag{20}$$

Its low-frequency asymptote matches Eq. (17). In the high-frequency limit, Eq. (20) replaces the divergence $\propto 1/\omega|K - \frac{1}{4}|$ of the $\delta'(\omega)$ terms in Eq. (12) and (18) with a nonanalytical factor $\propto (\ln\omega)/\omega$.

In general, the description of the full crossover between the low- and high-frequency asymptotes of the scaling function is a difficult problem. It can, however, be provided for the vicinity of the Schmid transition, $K = \frac{1}{2}$. Right at the transition, the Hamiltonian (8) can be mapped onto a tunnel Hamiltonian for free fermions [3]. In that case, the admittance is purely real and the frequency shift is purely imaginary, both being frequency independent. A small deviation from that point, $0 < \frac{1}{2} - K \ll 1$, corresponds to the case of weakly repulsive fermions in the leads [35]. Extending the theory developed in that reference to evaluate the interaction-induced corrections to the admittance and using its relation with the phase shift, we find

$$\tan\delta(\omega) = (i - 2\pi\delta K)\left(\frac{\omega}{\omega_\star}\right)^{-4\delta K}, \quad \delta K = K - \frac{1}{2}, \tag{21}$$

at any ω (see details of the derivation in Appendix C 5). As expected, Eq. (21) matches the previously found asymptotes, Eqs. (12) and (16).

From the asymptotes and exact results given above, we deduce that inelastic scattering, captured by $\delta''(\omega)$, becomes significant at ω near $\omega_\star$. Scattering is fully inelastic at the critical point, $K = \frac{1}{2} - 0$, in accordance with the exact results [36–38] treated in the scaling limit (see Appendix C 5). The appearance of a structure in $\delta(\omega)$ upon deviation of K from the critical point is given by Eq. (21). The observability of the scaling regime in the entire range $K < \frac{1}{2}$ requires that $\omega_\star \ll \sqrt{\lambda E_J}$. As λ varies exponentially with E_J/E_C, the observation of a scaling behavior in a broad dynamical range may pose a challenge for experiments.

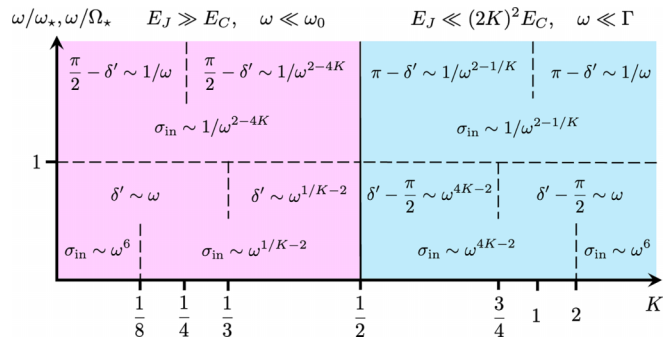

FIG. 2. High- and low-frequency asymptotes of $\delta'(\omega)$ and $\sigma_{\rm in}(\omega) = 1 - e^{-4\delta''(\omega)}$ in the scaling regime. For a transmon on the insulating side of the Schmid transition, $K < \frac{1}{2}$, the results are obtained from Eqs. (12), (16)–(18), and footnote [30]. The asymptotes for a charge qubit on the superconducting side of the transition, $K > \frac{1}{2}$, are obtained from these equations by the duality relation, see Eqs. (22), (6), and (7).

IV. FINITE-FREQUENCY RESPONSE OF A CIRCUIT TERMINATED BY A CHARGE QUBIT

Let us now turn to the opposite regime of the charge qubit. Starting from Hamiltonian (1) at $E_J \ll E_C$, we observe that its properties at frequencies below the cutoff Γ can be described by the same Hamiltonian (14) provided that one substitutes $\tilde{\lambda}$ with E_J in it. From that duality relation, we deduce that the scaling functions in Eqs. (6) and (7) are related,

$$f_{\rm qb}(\nu, K) = \frac{\pi}{2} + f_{\rm tr}\left(\nu, \frac{1}{4K}\right), \quad K > \frac{1}{2}, \tag{22}$$

provided that one uses the proper characteristic frequency scale for the charge qubit,

$$\Omega_\star = 2e^\gamma\Gamma\left(\frac{1}{\sqrt{2K\Gamma(1/K)}}\frac{\pi E_J}{2e^\gamma\Gamma}\right)^{2K/(2K-1)}, \quad K > \frac{1}{2}. \tag{23}$$

Here $\gamma \approx 0.58$ is Euler's constant [39]. To observe the entire crossover, one needs $\Omega_\star \ll \Gamma$, equivalent to $(2K)^2 E_C/E_J \gg 1$, in the entire interval $K > 1/2$. Overall, the constraint on $\Omega_\star$ is experimentally less challenging than the respective one for the transmon.

V. DISCUSSION

In conclusion, we developed a comprehensive theory of the dynamic response of a small Josephson junction in a high-impedance environment. The response is uniquely characterized by the complex-valued reflection phase $\delta(\omega)$. Its frequency dependence exhibits a nontrivial crossover with a functional form determined solely by the environmental impedance $\pi\hbar/4e^2K$. The low- and high-frequency asymptotes of $\delta(\omega)$ are summarized in Fig. 2. Depending on K, the low-frequency asymptote shows a capacitive or inductive

response, characteristic for an insulator or superconductor, respectively. The change between these two types of response occurs at $K = \frac{1}{2}$ (the Schmid transition point), irrespective of the values of the Josephson and charging energies (E_J and E_C) of the small junction. The ratio E_J/E_C, however, is important for the ability to observe the entire crossover function $\delta(\omega)$, see Fig. 2.

Short of observing the entire crossover in $\delta(\omega)$, the vestiges of the transition can be seen even in its high-frequency asymptote. This, to some extent was done in Ref. [8] by monitoring the real part $\delta'(\omega)$ of the reflection phase. The same experiment yielded the data for the dissipative part of the response $\delta''(\omega)$, too. The comparison of $\delta''(\omega)$ with our predictions is still outstanding [40].

Our paper also clearly shows that the data of Ref. [6] for a shunted SQUID are consistent with the existence of the Schmid transition. As one sees from our results, the flux tunability of the response is present even on the insulating side of the transition through the flux dependence of the crossover parameter $\omega_\star$. In the theoretical consideration presented in [6], the authors make a conceptual error by replacing the asymptotic behavior of the response function by an average value of $\cos\varphi$, which, being a quantity local in time, does not exhibit a quantum phase transition due to the low dimensionality of the system. The "average-cos φ" consideration is also one of the erroneous arguments against the Schmid transition presented in the numerical study [41]. The conclusions of this paper are at odds with the quantum Monte Carlo [42,43] and numerical RG [44] results. Other, technical errors of that paper were uncovered in [45]. We note here that Ref. [41] fails to reproduce even the simplest limit of an isolated transmon ($K \to 0$). We believe our paper helps to clarify the existing confusion regarding the Schmid transition and pave the way for experiments unambiguously demonstrating it.

Note added. Recently, we learned about a study [46] of the charge qubit limit, which was performed independently from our paper. The results of our two studies agree with each other, wherever comparable.

ACKNOWLEDGMENTS

We thank M. Goldstein for sending us the manuscript of [46] prior to making it public. M.H. thanks Yale University for hospitality, where this work was supported by NSF Grant No. DMR-2002275 and by ARO Grant No. W911NF-23-1-0051, as well as French CNRS IRP HYNATOQ and ANR-23-CE47-0004. T.Y. acknowledges support from JST Moonshot R&D-MILLENNIA Program (Grant No. JPMJMS2061).

APPENDIX A: RELATION BETWEEN SCATTERING PHASE AND CIRCUIT ADMITTANCE

Using the harmonic theory for a transmission line, we decompose the voltage and current nearby the junction in the circuit of Fig. 1 in terms of incoming and outgoing waves, $V_J(\omega) = V_{\rm in}(\omega) + V_{\rm out}(\omega)$ and $I(\omega) = [V_{\rm in}(\omega) - V_{\rm out}(\omega)]/R$, respectively. The transmission line realizes an ohmic impedance, such that $I(\omega) = [V(\omega) - V_J(\omega)]/R$. Defining the circuit admittance as $Y(\omega) = I(\omega)/V(\omega)$, we can relate it to the scattering phase $\delta(\omega)$ off the junction, such that $V_{\rm out}(\omega) = e^{2i\delta(\omega)}V_{\rm in}(\omega)$. As a result we get Eq. (3).

APPENDIX B: ADMITTANCE OF AN ALMOST ISOLATED TRANSMON, $K \to 0$

In this Appendix we show that the admittance of an isolated transmon is dominated at low frequency by the contribution of the quantum capacitance associated with it. Then, we determine the frequency shift of the modes in a transmission line weakly connected to the transmon, $K \ll 1$. Finally, we introduce a boundary sine-Gordon model that allows determining the response functions of the transmon's electromagnetic environment at any K. We use these results to discuss the structure of inelastic processes.

1. Quantum capacitance of an isolated Josephson junction

At $K = 0$, the junction is disconnected from the transmission line. The Hamiltonian (1) reduces to

$$H = E_J(1 - \cos\varphi) + 4E_C(N - \mathcal{N})^2. \tag{B1}$$

Here $\mathcal{N}$ is related with the current bias, $I = 2e\dot{\mathcal{N}}$. The inverse admittance $Y^{-1}_{K=0}$ is then defined as the ratio between the voltage $V_J = \langle\dot{\varphi}\rangle/2e$ and I. Using the equation of motion derived from Eq. (B1), $\dot{\varphi} = 8E_C(\mathcal{N} - N)$, and linear response, we find

$$Y^{-1}_{K=0}(\omega) = \frac{1}{-i\omega C}[1 + 8E_C G_{N,N}(\omega)], \tag{B2}$$

where $G_{N,N}(\omega)$ is the Fourier transform of the retarded Green's function $G_{N,N}(t) = -i\theta(t)\langle[N(t), N]\rangle$ evaluated at $\mathcal{N} = 0$. (Here we assume that an eventual static offset charge is screened by the junction's environment.) Using the transmon's eigenbasis of states $|s\rangle$ with energy ε_s, such that $\varepsilon_s < \varepsilon_{s'}$ for $0 \leqslant s < s'$, we express Eq. (B2) as

$$Y^{-1}_{K=0}(\omega) = \frac{1}{-4e^2 i\omega}\left[8E_c - \sum_{s>0}|W_{0s}|^2\frac{2\varepsilon_{s0}}{\varepsilon_{s0}^2 - \omega^2}\right] \tag{B3}$$

with $\varepsilon_{ss'} = \varepsilon_s - \varepsilon_{s'}$ and $W_{ss'} = 8E_C\langle s|N|s'\rangle$. We now use an identity obtained by evaluating perturbatively $\mathcal{N}$-dependent corrections to ε_s [25],

$$\frac{2e^2}{C_\star} \equiv \frac{1}{2}\frac{\partial^2\varepsilon_0}{\partial\mathcal{N}^2} = 4E_C - \sum_{s>0}\frac{|W_{0s}|^2}{\varepsilon_{s0}}, \tag{B4}$$

to find

$$Y^{-1}_{K=0}(\omega) = \frac{1}{-i\omega C_\star} - \frac{i\omega}{4e^2}\sum_{s>0}\frac{2|W_{0s}|^2}{\varepsilon_{s0}\left(\varepsilon_{s0}^2 - \omega^2\right)}. \tag{B5}$$

The most striking feature of Eq. (B5) is that the low-frequency response is dominated by the contribution of the quantum capacitance $C_\star$ at any ratio E_J/E_C. It illustrates the insulating behavior the junction at $\omega \to 0$, in accordance with Schmid's prediction.

In particular, in a transmon, $E_J \gg E_C$, $W_{0s} \approx -i8E_C(E_J/32E_C)^{1/4}\delta_{s,1}$ and $\varepsilon_{10} \approx \omega_0 = \sqrt{8E_J E_C}$. Thus the second term in Eq. (B5) reduces to the classical result for an inductance $L_J = 1/4e^2E_J$ in parallel with C. It is effectively inductive at $\omega < \omega_0$. According to Eq. (B5), the

quantum capacitance $C_\star$ appears in series with that effective inductance. Using

$$\varepsilon_0 = \tfrac{1}{2}\omega_0 - \lambda\cos(2\pi\mathcal{N}) \tag{B6}$$

with phase-slip amplitude λ given in Eq. (5), we find $C_\star = e^2/\pi^2\lambda$. (Here we evaluated $C_\star$ assuming again that an eventual offset charge is screened by a weakly coupled environment, see [47].)

The low-frequency response is also dominated by the capacitive term in a charge qubit, $E_J \ll E_C$, where $C_\star \approx C$ and the capacitive response extends in a wide frequency range of order E_C.

2. Frequency shift at $K \ll 1$

At $K \ll 1$, we find that $Y_J \approx Y_{K=0}$ can be used to evaluate the mode frequency shift of the q mode in a transmission line weakly connected to a Josephson junction. Indeed, expressing Eq. (1) at $\mathcal{N} = 0$ [47] in the transmon eigenbasis,

$$H = \sum_s \varepsilon_s|s\rangle\langle s| + \sum_q \omega_q a_q^\dagger a_q + 4E_c n^2 - n\sum_{ss'} W_{ss'}|s\rangle\langle s'|, \tag{B7}$$

and using perturbation theory up to order K, we find that $\delta\omega_q/\Delta = 1/i\pi R Y_{K=0}(\omega_q)$ in a wide frequency range $1/RC_\star \ll \omega_q \ll \varepsilon_{10}$ where $\delta\omega_q/\Delta \ll 1$. In particular, the correction $\delta\omega_q$ is dominated by the capacitive response, $\delta\omega_q/\Delta \approx 1/\pi RC_\star\omega_q$, in the frequency range $1/RC_\star \ll \omega_q \ll 1/\sqrt{L_J C_\star}$ in a transmon ($E_J \gg E_C$), and $1/RC_\star \ll \omega_q \ll E_C$ in a charge qubit ($E_J \ll E_C$). These results match Eq. (4) at large R (small K), when $\pi/2 - \delta(\omega) \ll 1$.

In the main text, we extrapolated the results to lower frequency, $\omega_q \ll 1/RC_\star$, using

$$\tan\delta(\omega) = \omega RC_\star. \tag{B8}$$

Equation (B8) is, however, beyond perturbation theory in K.

In the next subsection, we motivate the introduction of the boundary sine-Gordon model, Eq. (8), which allows extending the results at any K and ω.

3. Boundary sine-Gordon model

Further insight is obtained by evaluating the ground-state energy associated with the Hamiltonian (B7) perturbatively in K,

$$E_g = \varepsilon_0 + \sum_q \frac{K\Delta}{\pi^2\omega_q}\left[4E_C - \sum_s \frac{|W_{0s}|^2}{\varepsilon_{s0}+\omega_q}\right]. \tag{B9}$$

Here the second term yields an $\mathcal{N}$-dependent correction to E_g. Focussing on the transmon regime, we evaluate this term in logarithmic approximation after substracting Eq. (B4) to the factor between brakets. As a result, we find that the $\mathcal{N}$-dependent correction to E_g can be accounted by the substitution

$$\lambda \to \lambda[1 - 2K\ln(\omega_0/\omega_{\min})] \tag{B10}$$

in the expression for ε_0, cf. Eq. (B6). Here we used $\omega_{\min}$ to cutoff an IR divergency, while ω_0 appeared as the natural cutoff for the UV divergency.

This motivates us for describing the low-frequency response of a transmon at any K with a boundary sine-Gordon model [equivalent to Eq. (8)],

$$H_{\rm sG} = -\lambda\cos 2\pi(n+\mathcal{N}) + \sum_q \omega_q a_q^\dagger a_q, \tag{B11}$$

where ω_0 sets the bandwidth for the boson modes (up to a numerical prefactor beyond the accuracy of our considerations). Indeed, at $\mathcal{N} = 0$ this model yields a renormalization of the phase slip amplitude due to the environmental modes,

$$\lambda_{\rm eff} = \lambda(\omega_0/\omega_{\min})^{-2K}, \tag{B12}$$

in agreement the substitution rule (B10) at $K \ll 1$. The presence of $\omega_{\min}$ in that correction points to the fact that the term $\propto\lambda$ in Eq. (B11) is a relevant (irrelevant) perturbation at $K < \frac{1}{2}$ ($K > \frac{1}{2}$), see the main text.

4. Inelastic cross section

Following Ref. [25] we also evaluate the partial inelastic cross section for a photon with frequency $\omega \ll \varepsilon_{10}$ to be converted into three photons with frequencies $\omega_1, \omega_2, \omega_3$, such that $\omega = \omega_1 + \omega_2 + \omega_3$,

$$\gamma(\omega_1,\omega_2,\omega_3|\omega) = \frac{4\pi^2}{3!}\frac{K^4}{\pi^8\omega\omega_1\omega_2\omega_3}\left(\frac{\partial^4\varepsilon_0}{\partial\mathcal{N}^4}\right)^2. \tag{B13}$$

Here we used another identity similar to Eq. (B4),

$$\frac{1}{4!}\frac{\partial^4\varepsilon_0}{\partial\mathcal{N}^4} = \sum_{s,t>0}\frac{|W_{0s}|^2}{\varepsilon_{s0}}\frac{|W_{0t}|^2}{\varepsilon_{t0}^2} - \sum_{s,r,t>0}\frac{W_{0s}W_{sr}W_{rt}W_{t0}}{\varepsilon_{s0}\varepsilon_{r0}\varepsilon_{t0}}, \tag{B14}$$

to simplify an equation derived from Eq. (7) in [25] at $\omega, \omega_1, \omega_2, \omega_3 \ll \varepsilon_{10}$. The contribution of the three-photon processes to the inelastic cross section is then estimated as

$$\begin{aligned}\gamma^{(3)}(\omega) &= \int d\omega_1 \int d\omega_2 \gamma(\omega_1,\omega_2,\omega-\omega_1-\omega_2|\omega)\\ &\approx \frac{4\pi^2}{2!}\frac{2^8K^4\lambda^2}{\omega^2}\ln^2\frac{\omega}{\omega_{\min}}.\end{aligned} \tag{B15}$$

Here we evaluated the integrals in logarithmic approximation. Evaluating similarly all processes where an incident photon is converted into $2m+1$ photons, we find the corresponding cross section,

$$\gamma^{(2m+1)}(\omega) \approx \frac{4\pi^2}{(2m)!}\frac{(4K)^{2m+2}\lambda^2}{\omega^2}\ln^{2m}\frac{\omega}{\omega_{\min}}. \tag{B16}$$

The sum of all these processes yield the inelastic cross section,

$$\begin{aligned}\sigma_{\rm in}(\omega) &= \sum_{m=1}^{\infty}\gamma^{(2m+1)}(\omega)\\ &\approx \frac{64\pi^2K^2\lambda^2}{\omega^2}\left[\cosh\left(4K\ln\frac{\omega}{\omega_{\min}}\right) - 1\right]\\ &\approx \frac{32\pi^2K^2\lambda^2}{\omega^2}\left(\frac{\omega}{\omega_{\min}}\right)^{4K}\end{aligned} \tag{B17}$$

at $K\ln(\omega/\omega_{\min}) \gg 1$. Taking into account the renormalization of λ given by Eq. (B12) and expression (13) for the crossover

frequency at $K \ll 1$, we finally get

$$\delta''(\omega) = \frac{\sigma_{\rm in}(\omega)}{4} = \left(\frac{\omega_\star}{\omega}\right)^{2-4K}, \tag{B18}$$

in agreement with Eq. (12).

Similar to the resonance fluorescence studied in Ref. [25], the logarithmic factors in the partial inelastic cross sections, Eq. (B16), illustrate that an incident photon with frequency $\omega \gg \omega_\star$ is quasielastically scattered into another photon with slightly smaller frequency, as well an even number of low-frequency photons.

APPENDIX C: ADMITTANCE OF A TRANSMON WITHIN THE BOUNDARY SINE-GORDON MODEL

In this section we provide details on the derivation of the circuit admittance in the transmon regime.

1. Exact formula for the admittance

The Hamiltonian (B11) [Eq. (8)] is conveniently expressed as

$$H_{\rm sG} = \sum_q \frac{\omega_q}{2}\left(X_q^2 + P_q^2\right) - \lambda \cos 2\pi(n + \mathcal{N}), \tag{C1}$$

$$n = \frac{1}{\pi}\sum_q \sqrt{\frac{2K\Delta}{\omega_q}} X_q. \tag{C2}$$

Here we introduced the canonically conjugate variables $X_q = (a_q + a_q^\dagger)/\sqrt{2}$ and $P_q = (a_q - a_q^\dagger)/i\sqrt{2}$. Using linear response of the current, $I = 2e(\dot{n} + \dot{\mathcal{N}})$, to the applied bias, $V = 2eR\dot{\mathcal{N}}$, we express the admittance as

$$Y(\omega) = \frac{1}{R}[1 + 2\pi\lambda G_{n,\sin 2\pi n}(\omega)], \tag{C3}$$

where the Green's function is evaluated with Hamiltonian (C1) at $\mathcal{N} = 0$, and we used $G_{\dot{n},\sin 2\pi n}(\omega) = -i\omega G_{n,\sin 2\pi n}(\omega)$. Then we derive equivalent formulas for $Y(\omega)$ by using identities between various Green's functions. Indeed, using the equations of motion

$$\dot{X}_q = \omega_q P_q, \quad \dot{P}_q = -\omega_q X_q - 2\lambda\sqrt{\frac{2K\Delta}{\omega_q}}\sin 2\pi n, \tag{C4}$$

we find

$$G_{X_q,B}(\omega) = \frac{\sqrt{2K\Delta\omega_q}}{\omega^2 - \omega_q^2}\left[\frac{1}{\pi}\left\langle\frac{\partial B}{\partial n}\right\rangle + 2\lambda G_{\sin 2\pi n,B}(\omega)\right] \tag{C5}$$

for an arbitrary operator B expressed as a function of n only. Summing Green's functions with weights given by Eq. (C2) we find

$$G_{n,B}(\omega) = \frac{K}{i\omega}\left[\frac{1}{\pi}\left\langle\frac{\partial B}{\partial n}\right\rangle + 2\lambda G_{\sin 2\pi n,B}(\omega)\right], \tag{C6}$$

where we evaluated $\sum_q 2K\Delta/(\omega^2 - \omega_q^2) = \pi K/i\omega$ in the limit $\Delta \to 0$. (Recall that we consider retarded Green's functions, such that ω contains a small, positive imaginary part.) Using $B = n$ and $G_{n,\sin 2\pi n} = G_{\sin 2\pi n,n}$, and inserting the corresponding Eq. (C6) into Eq. (C3), we find $Y(\omega) = -4e^2 G_{\dot{n},n}(\omega)$. Using $B = \sin 2\pi n$, we also find

$$Y(\omega) = \frac{1}{R}[1 - 4\pi K\mathcal{G}(\omega)], \tag{C7}$$

$$\mathcal{G}(\omega) = \frac{\lambda^2}{-i\omega}[G_{\sin 2\pi n,\sin 2\pi n}(\omega) - G_{\sin 2\pi n,\sin 2\pi n}(\omega = 0)], \tag{C8}$$

in agreement with Eqs. (9) and (10). Here we used the relation

$$\langle\cos 2\pi n\rangle = -\lambda G_{\sin 2\pi n,\sin 2\pi n}(\omega = 0), \tag{C9}$$

which can be derived by evaluating perturbatively the response of $\langle\sin 2\pi(n + \mathcal{N})\rangle$, averaged over Eq. (B11), to a static $\mathcal{N}$ in two different ways: either we expand the operator to be quantum-averaged in $\mathcal{N}$, or we gauge out $\mathcal{N}$ form the operator into the Hamiltonian and, then, use linear response. Let us emphasize that Eq. (C7) is valid at any λ.

Equation (C7) allows establishing a relation between the admittance of the boundary sine-Gordon model and the conductance across an impurity in a Luttinger liquid [14,35]. Indeed, the first term in Hamiltonian (C1) may alternatively describe one-dimensional interacting fermionic leads. In that context, the parameter K characterizes whether the interactions between fermions are repulsive (at $K < \frac{1}{2}$) or attractive (at $K > \frac{1}{2}$). Using linear response, we then find that $e^2\mathcal{G}(\omega)$ in Eq. (C7) can be interpreted as the dynamical conductance of an electronic junction with tunnel current operator $\mathcal{I} = e\lambda\sin 2\pi(n + \mathcal{N})$ under voltage bias $\mathcal{V} = 2\pi\dot{\mathcal{N}}/e$.

2. Perturbation theory in λ at $K > \frac{1}{2}$

It is straightforward to evaluate the admittance up to order λ^2 with Eq. (C7). For this we just need to insert in it the low-frequency result for the Green's function $G_{\sin 2\pi n,\sin 2\pi n}(\omega)$ evaluated at $\lambda = 0$,

$$G_{\sin 2\pi n,\sin 2\pi n}(\omega) = \frac{-i\pi e^{-i2\pi K}}{2\Gamma(4K)\cos(2\pi K)}\frac{\omega^{4K-1}}{\omega_0^{4K}}, \quad \omega \ll \omega_0. \tag{C10}$$

In particular, at $K > \frac{1}{2}$, $G_{\sin 2\pi n,\sin 2\pi n}(\omega = 0) = 0$. The correction to $Y'(\omega) = 1/R$ remains small at any frequency [13,14]. It was noticed in a related context [13] that $Y''(\omega)$ is positive (inductive-like) at $\frac{1}{2} < K < \frac{3}{4}$ and diverges at $K = \frac{3}{4}$. The divergence signals an insufficiency of the low-energy model (B11). Indeed, at $K > \frac{3}{4}$ the power law in the ω dependence associated with the quantum response exceeds 1. This signals that the quantum response is superseded by the classical one [not accounted for in Eq. (B11)], $Y''(\omega) \simeq \omega L/R$, which also remains small up to a narrow vicinity of ω_0. Overall, the correction to $\delta(\omega) = \pi/2$ remains small at any frequency up to ω_0, as announced in the main text.

Let us remind here that perturbation theory is also fruitful to discuss the high-frequency regime at $K < \frac{1}{2}$, see the main text.

3. Dual model near the IR fixed point

At $K < \frac{1}{2}$, the boundary condition of the free bosonic field at the position of the impurity (the junction) changes

from $\partial_x\theta(0)=0$ to $\partial_x\varphi(0)=0$ (i.e., from von Neumann to Dirichlet condition as far as the θ field is concerned) between the UV fixed point corresponding to $\lambda=0$ in Eq. (8), and the IR fixed point corresponding to $\tilde\lambda=0$ in Eq. (14). To address the vicinity of the IR fixed point, it is convenient to introduce another set of bosonic annihilation/creation operators, $b_q=(x_q+ip_q)/\sqrt{2}$ and $b_q^\dagger=(x_q-ip_q)/\sqrt{2}$, such that Eq. (14) reads

$$H_{\rm dual}=\sum_q\frac{\omega_q}{2}\left(x_q^2+p_q^2\right)-\tilde\lambda\cos\varphi-\varphi\dot{\mathcal{N}},$$
$$\varphi=\sum_q\sqrt{\frac{2\Delta}{K\omega_q}}p_q. \tag{C11}$$

By linear response, the admittance is

$$Y(\omega)=\frac{1}{R}\left[1+\frac{K}{\pi}G_{\dot\varphi,\varphi}(\omega)\right], \tag{C12}$$

where the Green's function $G_{\dot\varphi,\varphi}(\omega)$ is evaluated with Eq. (C11) at $\mathcal{N}=0$. Similar to Appendix C 1, by using the equations of motion for x_q, p_q we find various identities between Green's functions and equivalent expressions for the admittance,

$$Y(\omega)=-\frac{\tilde\lambda}{R}G_{\varphi,\sin\varphi}(\omega)=4e^2\tilde{\mathcal{G}}(\omega), \tag{C13}$$
$$\tilde{\mathcal{G}}(\omega)=\frac{\tilde\lambda^2}{-i\omega}[G_{\sin\varphi,\sin\varphi}(\omega)-G_{\sin\varphi,\sin\varphi}(\omega=0)]. \tag{C14}$$

Here we used $\langle\cos\varphi\rangle=-\tilde\lambda G_{\sin\varphi,\sin\varphi}(\omega=0)$. Let us emphasize that all relations above are valid at any $\tilde\lambda$.

The term $\propto\tilde\lambda$ is an irrelevant perturbation near the IR fixed point. Therefore we may use the expression for $G_{\sin\varphi,\sin\varphi}(\omega)$ evaluated at $\tilde\lambda=0$ to evaluate the admittance up to order $\tilde\lambda^2$ down to the lowest frequencies. Noting that $G_{\sin\varphi,\sin\varphi}(\omega)$ can be read off the right-hand side of Eq. (C10) after the substitution $K\to1/4K$, and using Eq. (3) to convert the admittance into scattering phase shift, we readily find the low-frequency asymptote, Eq. (16).

Actually, as discussed in the main text, a series of additional perturbations,

$$V=\sum_{n>0}c_{2n}(\partial_x\theta(0))^{2n},\quad \partial_x\theta(0)=\sum_q\frac{\sqrt{K\Delta\omega_q}}{v}(b_q+b_q^\dagger), \tag{C15}$$

need to be added to the dual Hamiltonian (C11),

$$H_{sG}=H_{\rm dual}+V, \tag{C16}$$

in order to address the low-frequency response functions at $K<\frac{1}{3}$. The leading term $\propto c_2$ is quadratic in the θ field. Therefore it only contributes to elastic scattering. It yields a perturbative-in-c_2 contribution to the boson T matrix, $T_{qq'}=c_2K\Delta\sqrt{\omega_q\omega_q'}/v^2$ and, consequently, a linear-in-ω contribution to the elastic phase shift, $\delta(\omega)=-\pi c_2K\omega/v^2\ll1$ with $c_2<0$. This contribution with $\pi c_2K/v^2=-1/\beta(K)\omega_\star$ corresponds to the first term in the right-hand side of Eq. (17). To find the dependence of c_2 on the circuit parameters, we note that such a linear-in-ω phase shift corresponds to an additive contribution to the boson density of states,

$$\delta\nu=\frac{1}{\pi}\frac{d\delta(\omega)}{d\omega}=c_2K/v^2. \tag{C17}$$

Therefore the boundary induces an additive correction to the specific heat, which takes a simple form in one dimension, $\delta C/T=(\pi^2/3)\delta\nu=\pi/3\beta(K)\omega_\star$. We benefited from an exact result for $\delta C/T$ given in Eq. (5.23) of Ref. [28] to find the expression for $\beta(K)$ at $K<\frac{1}{3}$, which appears in Eq. (17). Alternatively we might have used the expression for c_2 given in Eq. (3.21) of Ref. [29]. (From the comparison with [28], we suspect that the exponent of the factor $2\sin\pi g$ is actually twice larger than indicated there.)

The quartic term $\propto c_4$ contributes to the inelastic scattering cross section,

$$\sigma_{\rm in}(\omega)=\frac{4\pi^2}{3!}\frac{c_4^2K^4}{v^8}\int_0^\omega d\omega_1\int_0^{\omega-\omega_1}d\omega_2\omega\omega_1\omega_2(\omega-\omega_1-\omega_2)$$
$$=\frac{\pi^2}{180}\frac{c_4^2K^4\omega^6}{v^8}. \tag{C18}$$

This inelastic contribution becomes dominant at $K<\frac{1}{8}$, as stated in [30]. Taking into account an aforementioned modification of Eq. (3.21) in Ref. [29], we find

$$\delta''(\omega)=\frac{\sigma_{\rm in}(\omega)}{4}=\eta(K)\left(\frac{\omega}{\omega_\star}\right)^6, \tag{C19}$$

where, in particular, $\eta(K)\propto K^2$ at $K\ll1$.

4. Toulouse point, $K=\frac{1}{4}$

At $K=\frac{1}{4}$ (Toulouse point), we use the mapping to a fermionic field,

$$\psi(x)=\sqrt{\frac{\omega_0}{2\pi v}}\gamma e^{2i\pi n(x)}=\frac{1}{\sqrt{2L}}\sum_k\psi_ke^{ikx}, \tag{C20}$$

where γ is a Majorana fermion ($\gamma^2=1$) and ω_0 is a bandwidth that is of the order of the initial cutoff, to express the Hamiltonian (C1) at $\mathcal{N}=0$ as [14,34]

$$H_{\rm sG}=\sum_k vk\psi_k^\dagger\psi_k+\frac{\lambda}{2}\sqrt{\frac{2\pi v}{\omega_0}}[\psi(0)-\psi^\dagger(0)]\gamma. \tag{C21}$$

As the Hamiltonian is quadratic, the dynamical conductance $e^2\mathcal{G}(\omega)$ associated with it is easily obtained. Inserting the result in Eq. (C7), one obtains

$$RY(\omega)=1+\frac{2\omega_\star}{i\pi\omega}\ln\left(1-\frac{i\pi\omega}{2\omega_\star}\right),\quad \omega_\star=\frac{\pi^2\lambda^2}{2\omega_0}. \tag{C22}$$

Equation (20) is readily obtained from this result using the relation between the admittance and scattering phase given in Eq. (3).

5. Weakly interacting fermions, $\frac{1}{2}-K\ll1$

Another mapping is possible at the free-fermion point, $K=\frac{1}{2}$ [3], by introducing two fermionic fields, ψ_R and ψ_L,

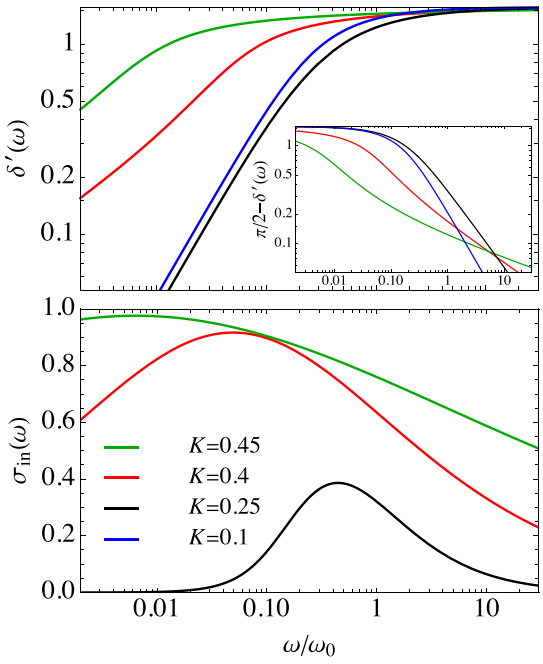

FIG. 3. Frequency dependence of $\delta'(\omega)$ and $\sigma_{\rm in}(\omega) = 1 - e^{-4\delta''(\omega)}$ for a transmon with $\lambda/\omega_0 = 0.2$ and various values of the environment impedance, using the classical result at $K = 0.1$, Eq. (20) at the Toulouse point, $K = 0.25$, and Eq. (21) at $K = 0.4$ and 0.45. (Upper panel) $\delta'(\omega)$ varies between 0 and $\pi/2$, and is plotted in log-log scale; (lower panel) $\sigma_{\rm in}(\omega)$ varies between 0 and 1, and is plotted in linear-log scale.

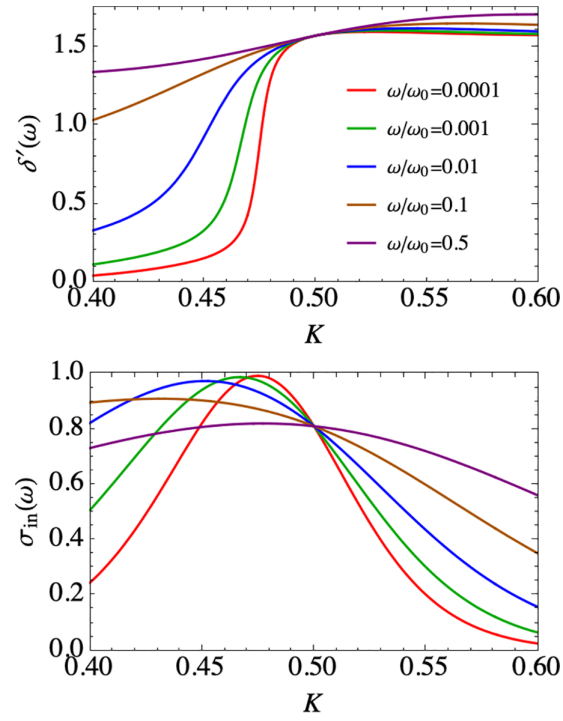

FIG. 4. Variation of δ' (upper panel) and $\sigma_{\rm in}$ (lower panel) as a function of K varying around the Schmid transition point, $K = \frac{1}{2}$, using Eq. (C25), for a set of fixed frequencies $\omega < \omega_0$, in a transmon with $\lambda/\omega_0 = 0.2$.

as in Eq. (C20). Then, Eq. (C1) at $\mathcal{N} = 0$ transforms into a conventional tunnel Hamiltonian,

$$H_{sG} = \sum_{k,\sigma=L,R} vk\psi^\dagger_{k\sigma}\psi_{k\sigma} + \frac{\pi v\lambda}{\omega_0}[\psi^\dagger_L(0)\psi_R(0) + \text{H.c.}]. \tag{C23}$$

The ω dependence of the tunnel conductance vanishes,

$$\mathcal{G} = \frac{1}{2\pi}\mathcal{T}, \quad \mathcal{T} = \frac{4(\pi\lambda/2\omega_0)^2}{[1 + (\pi\lambda/2\omega_0)^2]^2}. \tag{C24}$$

Thus $RY(\omega) = 1 - \mathcal{T} \equiv \mathcal{R}$ along the critical line $K = \frac{1}{2}$: the real part of the scattering phase vanishes and $\sigma_{\rm in} = 4\mathcal{T}(1-\mathcal{T})$.

The mapping of Eq. (C23) can be extended to arbitrary K by considering that the fermions in the leads are interacting. In particular, we may use the renormalization of the transmission amplitude found at weakly repulsive interaction, $0 < \frac{1}{2} - K \ll 1$, in Ref. [35] to find

$$RY(\omega) = \frac{1}{1 + (1 - i2\pi\delta K)(\omega/\omega_\star)^{4\delta K}}, \quad \delta K = K - \frac{1}{2}. \tag{C25}$$

Here $\omega_\star = \omega_0(\pi\lambda/\omega_0)^{1/(1-2K)}$, in agreement with Eq. (13) at $K \to \frac{1}{2}$. Note that the vanishing imaginary part in Eq. (C25) is found from the matching of $\delta(\omega)$ given in Eq. (21) [and obtained from Eq. (C25) and Eq. (3)], with its high- and low-frequency asymptotes, Eqs. (12) and (16), respectively.

From Eq. (C25) we find that $Y(\omega) \to 1/2R$ at $\omega = \omega_\star$ and $K \to \frac{1}{2} - 0$. Thus $\sigma_{\rm in}(\omega) \to 1$: scattering is fully inelastic. This result matches Eq. (C23) found at $K = \frac{1}{2}$ when one considers the scaling limit, $\omega_0 \to \infty$ with fixed $\omega_\star$, such that $\lambda/\omega_0 \simeq (\omega_\star/\omega_0)^{-2\delta K} \to 1$ and $\mathcal{T}, \mathcal{R} \to \frac{1}{2}$.

The results for the insulating side of the transition, $K < 1/2$, are illustrated by Fig. 3. Its upper panel shows the variation of the scattering phase by $\pi/2$ as the frequency ω passes the crossover value $\omega_\star$. The lower panel demonstrates a maximum of the inelastic photon scattering cross section at $\omega \sim \omega_\star$.

With the help of Eq. (C25), we illustrate also the evolution of the scattering phase shift across the Schmid transition in Fig. 4. The upper panel shows the variation of δ' as a function of K varying around $K = 1/2$ for a set of fixed frequencies $\omega < \omega_0$. The lower panel shows the variation of the inelastic scattering cross section $\sigma_{\rm in} = 1 - \exp(-4\delta'')$, which is a proxy for the dissipative part of the scattering phase shift, for the same range of K around $K = 1/2$ and for the same set of fixed frequencies. In each panel, all the curves representing different frequencies intersect at $K = 1/2$, indicating the transition point, see Eq. (C25). Another representative feature in the δ' vs K dependence at a fixed low frequency, is the increase of δ' by $\sim\pi/2$ with K increasing across the transition point.

[1] A. Schmid, Phys. Rev. Lett. **51**, 1506 (1983).

[2] S. A. Bulgadaev, Pisma Zh. Eksp. Teor. Fiz. **39**, 264 (1984) [JETP Lett. **39**, 315 (1984)].

[3] F. Guinea, V. Hakim, and A. Muramatsu, Phys. Rev. Lett. **54**, 263 (1985).

[4] R. Yagi, S. I. Kobayashi, and Y. Ootuka, J. Phys. Soc. Jpn. **66**, 3722 (1997).

[5] J. S. Penttilä, U. Parts, P. J. Hakonen, M. A. Paalanen, and E. B. Sonin, Phys. Rev. Lett. **82**, 1004 (1999).

[6] A. Murani, N. Bourlet, H. le Sueur, F. Portier, C. Altimiras, D. Esteve, H. Grabert, J. Stockburger, J. Ankerhold, and P. Joyez, Phys. Rev. X **10**, 021003 (2020).

[7] S. Léger, T. Sépulcre, D. Fraudet, O. Buisson, C. Naud, W. Hasch-Guichard, S. Florens, I. Snyman, D. M. Basko, and N. Roch, SciPost Phys. **14**, 130 (2023).

[8] R. Kuzmin, N. Mehta, N. Grabon, R. A. Mencia, A. Burshtein, M. Goldstein, and V. E. Manucharyan, arXiv:2304.05806.

[9] D. Subero, O. Maillet, D. S. Golubev, G. Thomas, J. T. Peltonen, B. Karimi, M. Marín-Suárez, A. Levy Yeyati, R. Sánchez, S. Park, and J. P. Pekola, Nat. Commun. **14**, 7924 (2023).

[10] M. P. A. Fisher and W. Zwerger, Phys. Rev. B **32**, 6190 (1985).

[11] U. Weiss and H. Grabert, Phys. Lett. A **108**, 63 (1985).

[12] S. E. Korshunov, Zh. Eksp. Teor. Fiz. **93**, 1526 (1987) [Sov. Phys. JETP **66**, 872 (1987)].

[13] C. Aslangul, N. Pottier, D. Saint-James, J. Phys. (Paris) **48**, 1093 (1987).

[14] C. L. Kane and M. P. A. Fisher, Phys. Rev. B **46**, 15233 (1992).

[15] F. Guinea, G. Gómez Santos, M. Sassetti, and M. Ueda, Europhys. Lett. **30**, 561 (1995).

[16] C. L. Kane and M. P. A. Fisher, Phys. Rev. Lett. **76**, 3192 (1996).

[17] J. Puertas Martínez, S. Léger, N. Gheeraert, R. Dassonneville, L. Planat, F. Foroughi, Y. Krupko, O. Buisson, C. Naud, W. Hasch-Guichard *et al.*, npj Quantum Inf. **5**, 19 (2019).

[18] R. Kuzmin, N. Mehta, N. Grabon, R. Mencia, and V. E. Manucharyan, npj Quantum Inf. **5**, 20 (2019).

[19] S. Léger, J. Puertas-Martínez, K. Bharadwaj, R. Dassonneville, J. Delaforce, F. Foroughi, V. Milchakov, L. Planat, O. Buisson, C. Naud *et al.*, Nat. Commun. **10**, 5259 (2019).

[20] R. Kuzmin, R. Mencia, N. Grabon, N. Mehta, Y.-H. Lin, and V. E. Manucharyan, Nat. Phys. **15**, 930 (2019).

[21] R. Kuzmin, N. Grabon, N. Mehta, A. Burshtein, M. Goldstein, M. Houzet, L. I. Glazman, and V. E. Manucharyan, Phys. Rev. Lett. **126**, 197701 (2021).

[22] N. Mehta, R. Kuzmin, C. Ciuti, and V. E. Manucharyan, Nature (London) **613**, 650 (2023).

[23] J. Koch, T. M. Yu, J. Gambetta, A. A. Houck, D. I. Schuster, J. Majer, A. Blais, M. H. Devoret, S. M. Girvin, and R. J. Schoelkopf, Phys. Rev. A **76**, 042319 (2007).

[24] Matching the result with the classical limit ($K \gg 1$) requires going beyond perturbation theory in λ, see Appendix C 2.

[25] M. Houzet and L. I. Glazman, Phys. Rev. Lett. **125**, 267701 (2020).

[26] A. Burshtein, R. Kuzmin, V. E. Manucharyan, and M. Goldstein, Phys. Rev. Lett. **126**, 137701 (2021).

[27] P. Fendley, A. W. W. Ludwig, and H. Saleur, Phys. Rev. B **52**, 8934 (1995).

[28] V. V. Bazhanov, S. L. Lukyanov, and A. B. Zamolodchikov, Commun. Math. Phys. **190**, 247 (1997).

[29] F. Lesage and H. Saleur, Nucl. Phys. B **546**, 585 (1999).

[30] Inelastic scattering ascribed to $\delta''(\omega)$ is given by the fractional power law in Eq. (17) down to $K = \frac{1}{8}$. At smaller K, a contribution $\propto (\omega/\omega_\star)^6$ takes over. It originates from the quartic term $\propto [\partial_x\theta(0)]^4$ that needs to be added to Eq. (14), see Appendix C 3.

[31] The remaining divergence $\propto \omega/|K - \frac{1}{3}|$ of the low-frequency asymptotes (16) and (17) likely reflects the critical behavior found in thermodynamic properties of the boundary sine-Gordon model at $K = \frac{1}{3}$ [32]. The frequency dependence associated with that critical behavior is currently not known.

[32] A. M. Tsvelik, J. Phys. A: Math. Gen. **28**, L625 (1995).

[33] V. Fateev, S. Lukyanov, A. Zamolodchikov, and A. Zamolodchikov, Phys. Lett. B **406**, 83 (1997).

[34] F. Guinea, Phys. Rev. B **32**, 7518 (1985).

[35] K. A. Matveev, D. Yue, and L. I. Glazman, Phys. Rev. Lett. **71**, 33511993.

[36] J. Polchinski and L. Thorlacius, Phys. Rev. D **50**, R622 (1994).

[37] C. G. Callan and I. R. Klebanov, Phys. Rev. Lett. **72**, 1968 (1994).

[38] C. G. Callan, R. Klebanov, A. W. W. Ludwig, and J. M. Maldacena, Nucl. Phys. B **422**, 417 (1994).

[39] U. Weiss, *Quantum Dissipative Systems* (World Scientific, Singapore, 2012).

[40] R. Kuzmin (private communication).

[41] K. Masuki, H. Sudo, M. Oshikawa, and Y. Ashida, Phys. Rev. Lett. **129**, 087001 (2022).

[42] P. Werner and M. Troyer, Phys. Rev. Lett. **95**, 060201 (2005).

[43] S. L. Lukyanov and P. Werner, J. Stat. Mech. (2007) P06002.

[44] A. Freyn and S. Florens, Phys. Rev. Lett. **107**, 017201 (2011).

[45] T. Sépulcre, S. Florens, and I. Snyman, Phys. Rev. Lett. **131**, 199701 (2023).

[46] A. Burshtein and M. Goldstein, arXiv:2308.15542.

[47] As discussed in [25], the large transmission line's capacitance, which grows linearly with its length, ensures that the zero mode not written in n of Eq. (2) would compensate for an eventual static offset charge $\mathcal{N}$.